

MICROCOPY RESOLUTION TEST CHART
NATIONAL BUREAU OF STANDARDS-1963-A

3

AD A1 25613



TECHNICAL REPORT RK-CR-82-11

RECENT ADVANCES IN COMBUSTION INSTABILITY ANALYSIS
FOR SOLID PROPELLANT ROCKET MOTORS

T. J. Chung
School of Science and Engineering
The University of Alabama in Huntsville
Huntsville, AL 35899

Prepared for:
Propulsion Directorate
US Army Missile Laboratory

RECEIVED
MAR 15 1983
A

May 1982



U.S. ARMY MISSILE COMMAND

Redstone Arsenal, Alabama 35809

Approved for public release; distribution unlimited.

DTIC FILE COPY

83 03 15 068

DISPOSITION INSTRUCTIONS

**DESTROY THIS REPORT WHEN IT IS NO LONGER NEEDED. DO NOT
RETURN IT TO THE ORIGINATOR.**

DISCLAIMER

**THE FINDINGS IN THIS REPORT ARE NOT TO BE CONSTRUED AS AN
OFFICIAL DEPARTMENT OF THE ARMY POSITION UNLESS SO DESIG-
NATED BY OTHER AUTHORIZED DOCUMENTS.**

TRADE NAMES

**USE OF TRADE NAMES OR MANUFACTURERS IN THIS REPORT DOES
NOT CONSTITUTE AN OFFICIAL INDORSEMENT OR APPROVAL OF
THE USE OF SUCH COMMERCIAL HARDWARE OR SOFTWARE.**

UNCLASSIFIED

SECURITY CLASSIFICATION OF THIS PAGE (When Data Entered)

REPORT DOCUMENTATION PAGE		READ INSTRUCTIONS BEFORE COMPLETING FORM
1. REPORT NUMBER RK-CR-82-11	2. GOVT ACCESSION NO. AD-A125 613	3. RECIPIENT'S CATALOG NUMBER
4. TITLE (and Subtitle) Recent Advances in Combustion Instability Analysis for Solid Propellant Rocket Motors		5. TYPE OF REPORT & PERIOD COVERED
7. AUTHOR(s) T. J. Chung		6. PERFORMING ORG. REPORT NUMBER
9. PERFORMING ORGANIZATION NAME AND ADDRESS Commander, US Army Missile Command ATTN: DRSMI-RK Redstone Arsenal, AL 35898		8. CONTRACT OR GRANT NUMBER(s) DAAH29-81-D-0100
11. CONTROLLING OFFICE NAME AND ADDRESS		10. PROGRAM ELEMENT, PROJECT, TASK AREA & WORK UNIT NUMBERS
14. MONITORING AGENCY NAME & ADDRESS (if different from Controlling Office)		12. REPORT DATE May 1982
		13. NUMBER OF PAGES 33
		15. SECURITY CLASS. (of this report) UNCLASSIFIED
		15a. DECLASSIFICATION/DOWNGRADING SCHEDULE
16. DISTRIBUTION STATEMENT (of this Report) Cleared for public release; distribution unlimited.		
17. DISTRIBUTION STATEMENT (of the abstract entered in Block 20, if different from Report)		
18. SUPPLEMENTARY NOTES		
19. KEY WORDS (Continue on reverse side if necessary and identify by block number) Vorticity, <input checked="" type="checkbox"/> Axisymmetric Coupled Acoustic Instability Vortex shedding Velocity Oscillations		
20. ABSTRACT (Continue on reverse side if necessary and identify by block number) Three-dimensional combustion stability integrals are derived with effects of viscosity and vorticity incorporated. For clarity of presentation, the particle distributions in gas dynamics are not considered at this time. It is suggested that the finite element method can be utilized to advantage for complicated geometries and boundary conditions. Some of the initial finite element calculations are demonstrated for an illustrative purpose, pending a full scale numerical applications in the future. (Author)		

DD FORM 1 JAN 73 1473

EDITION OF 1 NOV 65 IS OBSOLETE

UNCLASSIFIED

SECURITY CLASSIFICATION OF THIS PAGE (When Data Entered)

ACKNOWLEDGEMENTS

The assistance of Dr. R. M. Hackett and R. R. Radke of MICOM, and Mr. J. Y. Kim and Professor F. E. C. Culick of the University of Alabama, Huntsville is greatly appreciated. Appreciation is also expressed to the MICOM Propulsion Directorate, Redstone Arsenal, the Army Research Office, Durham, North Carolina, and Battelle Laboratories, Durham, for financial support of this project.



A

CONTENTS

	PAGE
1. INTRODUCTION	3
2. FORMULATION	4
3. THE STABILITY INTEGRAL	7
3.1 Vorticity-Coupled Acoustic Instability	7
3.2 Vorticity Stability Integral	16
4. FINITE ELEMENT ANALYSIS	18
5. APPLICATIONS	20
5.1 General	20
5.2 Vorticity-Uncoupled Acoustic Instability	24
5.3 Vorticity-Coupled Instability	
6. CONCLUSIONS	30

1. INTRODUCTION

Factors which contribute to the dissipation of acoustic energy in the chamber of solid rocket motors during combustion include - nozzle performance, particulate matter, propellant structural response, rotational flow, vortex shedding, etc. The most significant effect appears to be the response of the propellant combustion zone to acoustic pressure and acoustic velocity oscillations. A large body of literature exists relative to this subject, the study of which has been pioneered by Crocco [1], Cantrell and Hart [2], Culick [3,4], and others. Flandro and Jacobs [5], among others, have noted that vortex shedding can also lead to an excitation of pressure oscillations in solid propellant rocket motors. It is also quite possible that high speed mean flows affect the stability [6] significantly. Effects of transonic flow, shock waves, fluid viscosity at shear layers, turbulence, nonlinearity (second order perturbations), and radiation through high temperature should also be of concern.

The topics of study in this paper are limited to the basic question of correct stability integral formulation, and to three-dimensional finite element applications for stability calculations built upon the earlier work of Hackett [7]. Because of the flexibility of the finite element formulations, the present work can be extended, without difficulty, to a more general case incorporating various effects such as high speed flow, shock waves, particle and structural damping, turbulence, and radiation.

In what follows we present the formulation which includes consideration of vortex shedding and fluid viscosity. It has been shown that a simple and special case of the general formulation reduces to

the well-known results such as "flow turning" as well as "velocity and pressure coupling" terms. Numerical results of some simple geometries are discussed, pending a full scale computer code development based on the present formulation.

2. FORMULATION AND GOVERNING EQUATIONS

Consider a compressible, viscous fluid and the corresponding non-dimensional equations for continuity, momentum, energy, and state, as follows:

$$\frac{\partial \rho}{\partial t} + (\rho u_i)_{,i} = 0 \quad (1)$$

$$\rho \frac{\partial u_i}{\partial t} + \rho u_{i,j} u_j + \frac{1}{\gamma} p_{,i} - \frac{1}{Re} \left(u_{i,jj} + \frac{1}{3} u_{j,ji} \right) = 0 \quad (2)$$

$$\rho \frac{\partial T}{\partial t} - \frac{\gamma-1}{\gamma} \frac{\partial p}{\partial t} + \rho T_{,i} u_i - \frac{\gamma-1}{\gamma} p_{,i} u_i + \frac{\gamma(\gamma-1)}{Re} \left(\frac{2}{3} u_{i,i} u_{j,j} - u_{i,j} u_{j,i} - u_{j,i} u_{j,i} \right) = 0 \quad (3)$$

$$p = \rho T \quad (4)$$

where the commas denote partial derivatives, the repeated indices imply summing with the range of index i or j being 3. We use index notation in preference to vector symbols in order to facilitate clarification involved in integration by parts and computer coding in our later discussions. The nondimensional quantities are defined as:

$$u_i = \frac{\bar{u}_i}{a}, \quad a = \left(\frac{\gamma \bar{p}}{\bar{\rho}_0} \right)^{\frac{1}{2}}, \quad p = \frac{\bar{p}}{\bar{\rho}_0}, \quad T = \frac{C_p(\gamma-1)\bar{T}}{a^2},$$

$$x_i = \frac{\bar{x}_i}{L}, \quad t = \frac{a\bar{t}}{L}, \quad Re = \frac{\bar{\rho}_0 a L}{\mu}, \quad \rho = \frac{\bar{\rho}}{\bar{\rho}_0}$$

The presence of viscous terms is intended for development of shear layers close to the burning surface although the effect of viscosity is negligible in the flow domain with high Reynolds numbers.

Substituting Eqs. (1) and (4) into Eq. (3), we obtain

$$\frac{\partial p}{\partial t} + \gamma p u_{i,i} + p_{,i} u_i + \frac{\gamma^2}{Re} \left(\frac{2}{3} u_{i,i} u_{j,j} - u_{i,j} u_{j,i} - u_{j,i} u_{j,i} \right)$$

$$= 0 \quad (5)$$

To obtain the acoustic equation we take the spatial derivative of Eq. (2) and subtract the results from the time derivative of Eq. (5).

$$\frac{\partial^2 p}{\partial t^2} - \frac{p}{\rho} p_{,ii} = - \frac{\partial}{\partial t} (p_{,i} u_i) - \gamma \frac{\partial}{\partial t} (p u_{i,i}) + \gamma p \left[(u_{i,j} u_j)_{,i} \right]$$

$$- \frac{\gamma p}{\rho Re} \left[u_{i,jji} + \frac{1}{3} u_{j,jii} \right] - \frac{\gamma(\gamma-1)}{Re} \left\{ \frac{\partial}{\partial t} \left[\frac{2}{3} u_{i,i} u_{j,j} - u_{i,j} u_{j,i} \right. \right.$$

$$\left. \left. - u_{j,i} u_{j,i} \right] \right\} + \rho_{,i} \frac{\gamma p}{\rho} \left(\frac{\partial u_i}{\partial t} + u_{i,j} u_j \right) \quad (6)$$

At this point we introduce the perturbation expansion to $O(\epsilon)$ for the velocity u_i , pressure p , and density ρ in the form,

$$u_i = \bar{u}_i + \epsilon (u_i^* + u_i') \quad (7)$$

$$p = 1 + \epsilon p' \quad (8)$$

$$\rho = 1 + \epsilon \rho' \quad (9)$$

where the bar, asterisk, and prime denote the mean flow, vortical fluctuation, and acoustic fluctuation, respectively. Expanding Eq. (6) in terms of the perturbation variables and collecting the $O(\epsilon)$ terms, we

arrive at the expression:

$$\begin{aligned}
\frac{\partial^2 p'}{\partial t^2} - p'_{,ii} = & -\bar{u}_i \frac{\partial}{\partial t} p'_{,i} - \gamma \frac{\partial p'}{\partial t} \bar{u}_{i,i} + \gamma [\bar{u}_{i,j} u_j^* + \bar{u}_{i,j} u_j' \\
& + u_{i,j}^* \bar{u}_j + u_{i,j}' \bar{u}_j]_{,i} - \frac{\gamma}{Re} \left[(u_i^* + u_i'),_{jji} + \frac{1}{3} (u_j^* + u_j'),_{jii} \right] \\
& - \frac{2\gamma(\gamma-1)}{Re} \left\{ \frac{\partial}{\partial t} \left[\frac{2}{3} \bar{u}_{i,i} (u_j^* + u_j'),_j - \bar{u}_{i,j} (u_j^* + u_j'),_i \right. \right. \\
& \left. \left. - \bar{u}_{j,i} (u_j^* + u_j'),_i \right] \right\} \quad (10)
\end{aligned}$$

Considering the vorticity, defined as,

$$\varepsilon_{ijk} u_{k,j}^* = \xi_i^* \quad , \quad \varepsilon_{ijk} \bar{u}_{k,j} = \bar{\xi}_i \quad , \quad \xi_i = \bar{\xi}_i + \xi_i^* \quad (11)$$

the acoustic equation, Eq. (10), is recast in the form

$$p'_{,ii} - \frac{\partial^2 p'}{\partial t^2} = h \quad (12)$$

where

$$\begin{aligned}
h = & \bar{u}_i \frac{\partial p'_{,i}}{\partial t} + \gamma \frac{\partial p'}{\partial t} \bar{u}_{i,i} - \gamma \left[(\bar{u}_j u_j^*)_{,ii} + (\bar{u}_j u_j')_{,ii} - \varepsilon_{ijk} (\bar{u}_j \xi_k^* \right. \\
& \left. + u_j^* \bar{\xi}_k + u_j' \bar{\xi}_k)_{,i} \right] + \frac{\gamma}{Re} \left[(u_i^* + u_i'),_{jji} + \frac{1}{3} (u_j^* + u_j'),_{jii} \right] \\
& + \frac{2\gamma(\gamma-1)}{Re} \frac{\partial}{\partial t} \left[\frac{2}{3} \bar{u}_{i,i} (u_j^* + u_j'),_j - \bar{u}_{i,j} (u_j^* + u_j'),_i \right. \\
& \left. - \bar{u}_{j,i} (u_j^* + u_j'),_i \right] \quad (13)
\end{aligned}$$

with ε_{ijk} being the permutation symbol. The vorticity transport equation is obtained by taking a curl of the vector form of Eq. (2), and collecting the terms of $O(\varepsilon)$,

$$\frac{\partial \xi_i^*}{\partial t} - \varepsilon_{ijk} \varepsilon_{kmn} \left[\bar{u}_m \xi_n^* + (u_m^* + u_m') \bar{\xi}_n \right]_{,j} - \frac{1}{Re} \xi_{i,jj}^* = 0 \quad (14)$$

Equations (11), (12), and (14) represent the most general

vorticity-coupled acoustic problem in which the viscous action of the fluid is fully taken into account. Here the main objective is to determine the growth rate given by the stability integral. This subject is discussed in the following section.

3. THE STABILITY INTEGRAL

3.1 Vorticity-Coupled Acoustic Instability

To begin we must first consider the boundary conditions at the burning surface. In the direction normal to the surface, the momentum equation, Eq. (2), takes the form, in terms of $O(\epsilon)$,

$$-p'_{,i} n_i = f \quad (15)$$

with

$$f = \gamma \left\{ \frac{\partial}{\partial t} u'_i + (\bar{u}_j u'_j)_{,i} + (\bar{u}_j u'_j)_{,i} - \epsilon_{ijk} (\bar{u}_j \xi_k^* + u'_j \bar{\xi}_k + u'_j \bar{\xi}_k) \right. \\ \left. - \frac{1}{\text{Re}} \left[(u_i^* + u'_i)_{,jj} + \frac{1}{3} (u_j^* + u'_j)_{,ji} \right] \right\} n_i \quad (16)$$

The oscillatory motion of the acoustic media is modeled by

$$p' = \hat{p} e^{ikt} \quad (17a)$$

$$u'_i = \hat{u}_i e^{ikt}, \quad u_i^* = \hat{u}_i^* e^{ikt} \quad (17b)$$

$$\xi_i^* = \hat{\xi}_i^* e^{ikt} \quad (17c)$$

where k is the complex dimensionless frequency given by

$$k = \omega - i\alpha \quad (18)$$

Here, the imaginary part is known as the growth rate. The instability of acoustic pressure is signified by the growth of α proportional to $e^{\alpha t}$.

Substituting Eq. (17) into Eqs.(12)and (15) yields, respectively,

$$\begin{aligned}
 \hat{h} = & ik\bar{u}_{i,i}\hat{p}_{,i} + ik\gamma\bar{u}_{i,i}\hat{p} - \gamma\left[(\bar{u}_j \hat{u}_j^*),_{ii} + (\bar{u}_j \hat{u}_j'),_{ii} - \epsilon_{ijk} (\bar{u}_j \hat{\xi}_k^* + \hat{u}_j^* \bar{\xi}_k \right. \\
 & \left. + \hat{u}_j' \bar{\xi}_k),_{ii}\right] + \frac{\gamma}{\text{Re}}\left[(\hat{u}_i^* + \hat{u}_i'),_{jji} + \frac{1}{3}(\hat{u}_j^* + \hat{u}_j'),_{jii}\right] \\
 & + \frac{2ik\gamma(\gamma-1)}{\text{Re}}\left[\frac{2}{3}\bar{u}_{i,i}(\hat{u}_j^* + \hat{u}_j'),_{jj} - \bar{u}_{i,j}(\hat{u}_j^* + \hat{u}_j'),_{ii} \right. \\
 & \left. - \bar{u}_{j,i}(\hat{u}_j^* + \hat{u}_j'),_{ii}\right] \quad (19)
 \end{aligned}$$

and

$$\begin{aligned}
 \hat{f} = & \gamma\left\{ ik\hat{u}_i' + (\bar{u}_j \hat{u}_j^*),_{ii} + (\bar{u}_j \hat{u}_j'),_{ii} - \epsilon_{ijk} (\bar{u}_j \hat{\xi}_k^* + \hat{u}_j^* \bar{\xi}_k \right. \\
 & \left. + \hat{u}_j' \bar{\xi}_k) - \frac{1}{\text{Re}}\left[(\hat{u}_i^* + \hat{u}_i'),_{jj} + \frac{1}{3}(\hat{u}_j^* + \hat{u}_j'),_{jii}\right]\right\}_{,ii} \quad (20)
 \end{aligned}$$

The foregoing process leads to a nonhomogeneous Helmholtz equation

$$\hat{p}_{,ii} + k^2\hat{p} = \hat{h} \quad (21)$$

subject to the boundary condition

$$\hat{p}_{,i}n_i = -\hat{f} \quad (22)$$

For the solution of Eq. (21) we make use of the Green's function

[8]. It can easily be shown that

$$(k^2 - k_N^2)E_N^2 = \int_{\Omega} \hat{h} \hat{p}_N d\Omega + \int_{\Gamma} \hat{f} \hat{p}_N d\Gamma \quad (23)$$

where the unperturbed mode shape \hat{p}_N and the wave number k_N are determined from the classical acoustic problem,

$$\hat{p}_{N,ii} + k^2\hat{p}_N = 0 \quad (24)$$

$$\hat{p}_{N,i}n_i = 0 \quad (25)$$

Note that E_N^2 is given by the integral

$$E_N^2 = \int_{\Omega} \hat{p}_N^2 d\Omega \quad (26)$$

It should be noted that a correct integration of the right-hand side of Eq. (23) is the most crucial aspect of the present study. That is, integration by parts must be carried out until all Neumann boundary conditions are brought to the surface. Since \hat{h} in Eq. (19) contains the terms from the momentum equation differentiated once, it is now necessary that they be integrated by parts twice in order to produce the Neumann boundary conditions. For example, consider a single term taken from Eq. (19) substituted in Eq. (23) and integrated by parts:

$$\int_{\Omega} (\hat{u}_j \bar{u}_j)_{,ii} \hat{p}_N d\Omega = \int_{\Gamma} (\hat{u}_j \bar{u}_j)_{,i} n_i \hat{p}_N d\Gamma - \int_{\Omega} (\hat{u}_j \bar{u}_j)_{,i} \hat{p}_{N,i} d\Omega \quad (27a)$$

Integrating by parts now the second term of Eq. (27a) yields

$$-\int_{\Omega} (\hat{u}_j \bar{u}_j)_{,i} \hat{p}_{N,i} d\Omega = -\int_{\Gamma} \hat{u}_j \bar{u}_j n_i \hat{p}_{N,i} d\Gamma + \int_{\Omega} \hat{u}_j \bar{u}_j \hat{p}_{N,ii} d\Omega \quad (27b)$$

In order to demonstrate the advantage of tensor notations over vector notations in the process of integrations by parts, we consider a following example (eighth term of Eq. (19) substituted in Eq. (23)).

$$\begin{aligned} \int_{\Omega} u_{i,jj} \hat{p}_N d\Omega &= \int_{\Gamma} u_{i,jj} n_i \hat{p}_N d\Gamma - \int_{\Omega} u_{i,jj} \hat{p}_{N,i} d\Omega \\ &= \int_{\Gamma} u_{i,jj} n_i \hat{p}_N d\Gamma - \int_{\Gamma} u_{i,j} n_j \hat{p}_{N,i} d\Gamma + \int_{\Omega} u_{i,j} \hat{p}_{N,ij} d\Omega \end{aligned} \quad (28a)$$

If we pursue the above process in vector notations, we will encounter difficulty in obtaining the last term of Eq. (28a). To see this we begin with

$$\begin{aligned} \int_{\Omega} \nabla \cdot \nabla^2 u \hat{p}_N d\Omega &= \int_{\Gamma} \underline{n} \cdot \nabla^2 u \hat{p}_N d\Gamma - \int_{\Omega} \nabla^2 u \cdot \nabla \hat{p}_N d\Omega \\ &= \int_{\Gamma} \underline{n} \cdot \nabla^2 u \hat{p}_N d\Gamma - \int_{\Gamma} (\underline{n} \cdot \nabla) u \cdot \nabla \hat{p}_N d\Gamma + \int_{\Omega} (?) d\Omega \end{aligned} \quad (28b)$$

In integrating by parts $\int_{\Omega} \nabla^2 \underline{u} \cdot \underline{\nabla} \hat{p}_N d\Omega$, only the boundary term can be obtained in vector notations. To obtain the domain term, the quantity $\nabla^2 \underline{u} \cdot \underline{\nabla} \hat{p}_N$ must be expanded into individual terms. Other than in special cases such as this, however, the vector notations can be used to perform integration by parts. But care must be exercised to ensure correct product operations.

An evaluation of the rest of the integrals in Eq. (23) leads to

$$\begin{aligned}
& (k^2 - k_N^2) E_N^2 = i\gamma k_N \int_{\Gamma} \hat{u}'_i \hat{p}_{N,i} n_i d\Gamma + ik_N (\gamma + 1) \int_{\Gamma} \bar{u}_i \hat{p}_{N,i}^2 n_i d\Gamma - ik_N \int_{\Omega} \bar{u}_{i,i} \hat{p}_N^2 d\Omega \\
& - ik_N (2\gamma + 1) \int_{\Omega} \bar{u}_i \hat{p}_N \hat{p}_{N,i} d\Omega + \gamma \int_{\Gamma} \bar{u}_j (\hat{u}_j^* + \hat{u}_j') p_{N,i} n_i d\Gamma - \gamma \int_{\Omega} \bar{u}_j (\hat{u}_j^* + \hat{u}_j') p_{N,ii} d\Omega \\
& - \gamma \int_{\Omega} \epsilon_{ijk} (\bar{u}_j \hat{\xi}_k + \hat{u}_j^* \bar{\xi}_k + \hat{u}_j' \bar{\xi}_k) p_{N,i} d\Omega \\
& - \frac{\gamma}{\text{Re}} \int_{\Gamma} [(\hat{u}_i^* + \hat{u}_i'),_j \hat{p}_{N,i} n_j + \frac{1}{3} (\hat{u}_j^* + \hat{u}_j'),_j p_{N,i} n_i] d\Gamma \\
& + \frac{\gamma}{\text{Re}} \int_{\Omega} [(\hat{u}_i^* + \hat{u}_i'),_j \hat{p}_{N,ij} + \frac{1}{3} (\hat{u}_j^* + \hat{u}_j'),_j \hat{p}_{N,ii}] d\Omega \\
& + \frac{2ik\gamma(\gamma-1)}{\text{Re}} \int_{\Omega} \left[\frac{2}{3} \bar{u}_{i,i} (\hat{u}_j^* + \hat{u}_j'),_j - \bar{u}_{i,j} (\hat{u}_j^* + \hat{u}_j'),_i \right. \\
& \left. - \bar{u}_{j,i} (\bar{u}_j^* + \hat{u}_j'),_i \right] \hat{p}_N d\Omega \tag{29}
\end{aligned}$$

Note that, in view of our choice made in Eq. (25), we set $\hat{p} = \hat{p}_N$ and $k = k_N$ in Eqs. (19) and (20). Squaring both sides of Eq. (18) and in view of $\omega = \omega_N = k_N$ at $\alpha = 0$ for neutral stability, we obtain

$$k^2 - k_N^2 = -i2\alpha k_N + \alpha^2 \tag{30}$$

Comparing Eq. (30) with Eq. (29), we may solve for the growth rate α ($\alpha^2 \ll |2\alpha K_N|$) by equating the imaginary parts,

$$\begin{aligned}
 \alpha = & -\frac{1}{2E_N^2} \left[\int_{\Gamma} \left\{ \underbrace{\gamma \hat{u}_i^{(R)} \hat{p}_{N,i} n_i}_{(A)} + (\gamma+1) \bar{u}_i \hat{p}_N^2 n_i + \frac{\gamma}{k_N} \bar{u}_j \left(\hat{u}_j^* + \hat{u}_j \right)^{(I)} \hat{p}_{N,i} n_i}_{(B)} \right. \right. \\
 & - \frac{\gamma}{k_N \text{Re}} \left[\left(\hat{u}_i^* + \hat{u}_i \right)_{,j}^{(I)} \hat{p}_{N,i} n_j + \frac{1}{3} \left(\hat{u}_j^* + \hat{u}_j \right)_{,j}^{(I)} \hat{p}_{N,i} n_i \right] \left. \right\} d\Gamma \\
 & + \int_{\Omega} \left\{ \underbrace{-\bar{u}_{i,i} \hat{p}_N^2 - (2\gamma+1) \bar{u}_i \hat{p}_N \hat{p}_{N,i}}_{(D)} - \frac{\gamma}{k_N} \left[\bar{u}_j \left(\hat{u}_j^* + \hat{u}_j \right)^{(I)} \hat{p}_{N,ii} \right. \right. \\
 & \left. \left. - \epsilon_{ijk} \left(\bar{u}_j \hat{\xi}_k + \hat{u}_j^* \bar{\xi}_k + \hat{u}_j \bar{\xi}_k \right)^{(I)} \hat{p}_{N,i} \right] \right. \\
 & \left. + \frac{\gamma}{k_N \text{Re}} \left[\left(\hat{u}_i^* + \hat{u}_i \right)_{,j}^{(I)} \hat{p}_{N,ij} + \frac{1}{3} \left(\hat{u}_j^* + \hat{u}_j \right)_{,j}^{(I)} \hat{p}_{N,ii} \right] \right. \\
 & \left. \left. + \frac{2\gamma(\gamma-1)}{\text{Re}} \left[\frac{2}{3} \bar{u}_{i,i} \left(\hat{u}_j^* + \hat{u}_j \right)_{,j}^{(R)} - \bar{u}_{i,j} \left(\hat{u}_j^* + \hat{u}_j \right)_{,i}^{(R)} \right. \right. \right. \\
 & \left. \left. \left. - \bar{u}_{j,i} \left(\hat{u}_j^* + \hat{u}_j \right)_{,i}^{(R)} \right] \hat{p}_N \right\} d\Omega \right] \quad (31)
 \end{aligned}$$

where the superscripts (R) and (I) refer to the real and imaginary parts, respectively, and the various terms are defined as:

- (A) Surface combustion
- (B) Surface convection
- (C) Surface viscous damping
- (D) Combustion into domain
- (E) Convection into domain
- (F) Momentum viscous damping
- (G) Dissipative energy

It should be noted that the mean flow vorticity $\bar{\xi}_i$, the vortical fluctuation $\hat{\xi}_i$, and the vortical component of the velocity \hat{u}_i^* must be known in order to evaluate the integral, which we shall discuss in Section 3.2. It is possible, however, to evaluate the stability integral in an alternative form without explicit values of the vorticity. To this end, we proceed with the convective term $(\underline{u} \cdot \nabla)\underline{u}$ instead of $\nabla(\frac{1}{2} u^2) - \underline{u} \times \underline{\xi}$. Thus we return to Eq. (23) and examine the integral of the form

$$\int_{\Omega} \nabla \cdot (\underline{u} \cdot \nabla) \underline{u} \hat{p}_N d\Omega = \int_{\Omega} (\underline{u}_{i,j} \underline{u}_j)_{,i} \hat{p}_N d\Omega \quad (32)$$

Integrating Eq. (32) by parts twice, we obtain the growth rate similar to Eq. (31) except that the terms designated as (B) and (E) are replaced by

$$\alpha_{(B)} = -\frac{1}{2E_N^2} \int_{\Gamma} \frac{\gamma}{k_N} \left[\bar{u}_i (\hat{u}_j^* + \hat{u}'_j)^{(I)} + (\hat{u}_i^* + \hat{u}'_i)^{(I)} \bar{u}_j \right] \hat{p}_{N,i} n_j d\Gamma \quad (33a)$$

$$\alpha_{(E)} = -\frac{1}{2E_N^2} \int_{\Omega} -\frac{\gamma}{k_N} \left\{ \left[\bar{u}_i (\hat{u}_j^* + \hat{u}'_j)_{,j} \right]^{(I)} + (\hat{u}_i^* + \hat{u}'_i)^{(I)} \bar{u}_{j,j} \right\} \hat{p}_{N,i} + \left[\bar{u}_i (\hat{u}_j^* + \hat{u}'_j)^{(I)} + (\hat{u}_i^* + \hat{u}'_i)^{(I)} \bar{u}_j \right] \hat{p}_{N,i,j} \Big\} d\Omega \quad (33b)$$

A careful examination of the integrals above is in order. Recall that the counterparts of $\alpha_{(B)}$ and $\alpha_{(E)}$ in Eq. (31) were obtained from

$$\int_{\Omega} \nabla \cdot \left[\nabla \left(\frac{1}{2} u^2 \right) - \underline{u} \times \underline{\xi} \right] \hat{p}_N d\Omega = \int_{\Omega} \left[(\underline{u}_j \underline{u}_j)_{,ii} - \epsilon_{ijk} \xi_{k,ji} \right] \hat{p}_N d\Omega \quad (34)$$

The vorticity can be easily removed from Eq. (34) by setting $\underline{\xi} = 0$. This can not be done in the case of Eq. (32). The vortical component \hat{u}^* can be set equal to zero in both Eqs. (32) and (34) with $\underline{\xi} = 0$ in Eq. (34), but this will not

make both equations equivalent. In other words, the effect of irrotationality cannot be assured from Eq. (32) simply by setting $\hat{u}^* = 0$, and we are aware that

$$[(\bar{u} + \varepsilon \hat{u}') \cdot \nabla](\bar{u} + \varepsilon \hat{u}') \neq \nabla \left[\frac{1}{2} (\bar{u} + \varepsilon \hat{u}') \cdot (\bar{u} + \varepsilon \hat{u}') \right]$$

If the viscous effect is neglected, then the terms designated by (C), (F), and (G) will be eliminated. Thus

$$\alpha = -\frac{1}{2E_N^2} [(A) + (B) + (D) + (E)] \quad (35)$$

Evaluation of the integrals given by Eqs. (31) and (35) requires adequate analytical or numerical models for the mean flow and vortical and acoustic components of the velocity. These topics will be discussed in Section 5.

If we assume $\xi_i = 0$, $\hat{u}_i^* = 0$, and $Re \rightarrow \infty$ in Eq. (31), we obtain

$$\begin{aligned} (\alpha_a)_{\xi_i=0} = & -\frac{1}{2E_N^2} \left[\int_{\Gamma} \left[\gamma \hat{u}_i^{(R)} \hat{p}_{N,i} n_i + (\gamma + 1) \bar{u}_i \hat{p}_{N,i}^2 n_i \right. \right. \\ & + \frac{\gamma}{k_N} \bar{u}_j \hat{u}_j^{(I)} \hat{p}_{N,i} n_i \left. \right] d\Gamma + \int_{\Omega} \left[-\bar{u}_{i,i} \hat{p}_{N,i}^2 - (2\gamma + 1) \bar{u}_i \hat{p}_{N,i} \right. \\ & \left. \left. - \frac{\gamma}{k_N} \bar{u}_j \hat{u}_j^{(I)} \hat{p}_{N,i} \right] d\Omega \right] \quad (36) \end{aligned}$$

Here the velocity normal to the boundary surface is expressed in terms of the admittance, $A = A^{(R)} + iA^{(I)}$, and the mean flow Mach number \bar{M} such that

$$\hat{u}'_i n_i = (\hat{u}_i^{(R)} + i \hat{u}_i^{(I)}) n_i = \bar{M} A \hat{p}_{N,i} / \gamma \quad (37)$$

whereas the acoustic fluctuation velocity in the domain is given by

$$\hat{u}'_i = \frac{i}{k_N \gamma} \hat{p}_{N,i} \quad (38)$$

Invoking the relationships of Eqs. (24) and (25) and setting $\bar{u}_{i,i} = 0$ (incompressible flow), one obtains

$$(\alpha_a)_{\xi_{i=0}} = - \frac{1}{2E_N^2} \int_{\Gamma} \left[\gamma \hat{u}_i^{(R)} n_i \hat{p}_N + \bar{u}_i \hat{p}_N^2 n_i \right] d\Gamma \quad (39)$$

which is the familiar expression as derived by Culick [see Eq. (2.29) of Ref. 4 neglecting particle distributions]. This is the simplest form representing the possible unstable motions in a solid propellant rocket motor. It has the ingredients such as velocity coupling (burning rate changes in response to velocity fluctuations parallel to the surface) and pressure coupling (burning rate changes in response to pressure fluctuations on the surface).

Culick, [3,4] further defines the "flow turning" as an averaged approximation to viscous effects which appeared in one-dimensional analysis but did not arise in the three-dimensional inviscid flow. This claim has also been substantiated by the present authors as shown in Eq. (39).

Let us now investigate the terms which result from Eq. (33a,b). The stability integral for the case of $Re \rightarrow \infty$ assumes the form

$$\begin{aligned} \alpha_a = - \frac{1}{2E_N^2} \left\{ \int_{\Gamma} \left[\gamma \hat{u}_i^{(R)} \hat{p}_N n_i + (\gamma+1) \bar{u}_i \hat{p}_N^2 n_i \right. \right. \\ + \frac{\gamma}{k_N} \left(\bar{u}_i \hat{u}_j^{(I)} + \hat{u}_i^{(I)} \bar{u}_j \right) \hat{p}_{N,i} n_j \left. \right] d\Gamma \\ + \int_{\Omega} \left[- \bar{u}_{i,i} \hat{p}_N^2 - (2\gamma+1) \bar{u}_i \hat{p}_N \hat{p}_{N,i} - \frac{\gamma}{k_N} \left(\bar{u}_i \hat{u}_{j,j}^{(I)} + \hat{u}_i^{(I)} \bar{u}_{j,j} \right) \hat{p}_{N,i} \right. \\ \left. + \left(\bar{u}_i \hat{u}_j^{(I)} + \hat{u}_i^{(I)} \bar{u}_j \right) \hat{p}_{N,ij} \right] d\Omega \right\} \quad (40) \end{aligned}$$

Now, using the relation given by Eq. (38), we have

$$\begin{aligned}
 \alpha_a = & -\frac{1}{2E_N^2} \left\{ \int_{\Gamma} \left[\gamma \hat{u}_i^{(R)} \hat{p}_N n_i + (\gamma+1) \bar{u}_i \hat{p}_N^2 n_i \right. \right. \\
 & + \frac{1}{k_N^2} (\bar{u}_i P_{N,j} P_{N,i} + \bar{u}_j P_{N,i} P_{N,i}) n_j \left. \right] d\Gamma \\
 & + \int_{\Omega} \left[-\bar{u}_{i,i} \hat{p}_N^2 - (2\gamma+1) \bar{u}_i \hat{p}_N \hat{p}_{N,i} - \frac{1}{k_N^2} (\bar{u}_i \hat{p}_{N,jj} \hat{p}_{N,i} \right. \\
 & \left. \left. + \bar{u}_{j,j} \hat{p}_{N,i} \hat{p}_{N,i} + \bar{u}_i \hat{p}_{N,j} \hat{p}_{N,ij} + \bar{u}_j \hat{p}_{N,i} \hat{p}_{N,ij}) \right] d\Omega \right\} \quad (41)
 \end{aligned}$$

For $\bar{u}_{i,i} = 0$, and using Eqs. (24) and (25), we obtain

$$\begin{aligned}
 \alpha_a = & -\frac{1}{2E_N^2} \left[\int_{\Gamma} \left(\gamma \hat{u}_i^{(R)} n_i \hat{p}_N + \bar{u}_i \hat{p}_N^2 n_i + \frac{1}{k_N^2} \bar{u}_j \hat{p}_{N,i} \hat{p}_{N,i} n_j \right) d\Gamma \right. \\
 & \qquad \qquad \qquad (A-1) \qquad \qquad \qquad (A-2) \qquad \qquad \qquad (B) \\
 & \left. + \frac{1}{k_N^2} \int_{\Omega} (\bar{u}_i \hat{p}_{N,j} \hat{p}_{N,ij} + \bar{u}_j \hat{p}_{N,i} \hat{p}_{N,ij}) d\Omega \right] \quad (42) \\
 & \qquad \qquad \qquad (D)
 \end{aligned}$$

According to Culick [3,4], the first two boundary terms are defined as combustion (at surface) and the last boundary term is known as the mean flow/acoustic interaction or "flow turning". Note that the "flow turning" term has appeared from the integration of Eq. (32) by parts "twice". The boundary term which results from the first integration cancels with a term from a boundary integral of Eq. (23). Upon integrating by parts "once more", we obtained the boundary terms in Eq. (33a) which finally led to the "flow turning" term. Recall that it arises from the convective term of the momentum equation. The same term, designated as "B" in Eq. (31) was called "surface convection". Conversely, the domain terms arising from

the convective terms of the momentum equation, designated as "D", were called "Convection into domain". These convection terms correspond to the popular definition of the "flow turning" as a consequence of injecting mass into the acoustic wave, which must supply acoustic energy to the mass in order that it be brought up to the local velocity [3,4]. Such action must combine both surface and domain integrals, linking the surface activities into the domain.

3.2 Vorticity Stability Integral

Recall that the coupling of vorticity with an acoustic field given by Eq. (31) is yet to be evaluated from the acceptable velocity profile in the shear layer. The influence of direct acoustic feedback and presence of unstable shear flow are to be taken into account.

One option for the solution is to establish an independent stability integral for vorticity. To this end, we return to Eqs. (14), (17b), and (17c), and write

$$\frac{i}{\text{Re}} \hat{\xi}_{i,jj}^* + k \hat{\xi}_i^* = \hat{H}_i \quad (43)$$

where

$$\hat{H}_i = -i \varepsilon_{ijk} \varepsilon_{kmn} \left[\bar{u}_m \hat{\xi}_n^* + (\hat{u}_m^* + \hat{u}_m') \bar{\xi}_n \right]_{,j} \quad (44)$$

subject to the boundary condition

$$\frac{i}{\text{Re}} \hat{\xi}_{i,j}^* n_j = -\hat{F}_i$$

It is evident that Eq. (43) represents diffusive waves due to production of vortex streets, and that the state of instability is once again determined from the Green's function technique [8]. It can easily be shown that

$$(k - k_N) D_N^2 = \int_{\Omega} \hat{H}_i \hat{\xi}_i^{*N} d\Omega + \int_{\Gamma} \hat{F}_i \hat{\xi}_i^{*N} d\Gamma \quad (45)$$

where

$$D_N^2 = \int_{\Omega} \hat{\xi}_i^N \hat{\xi}_i^N d\Omega = \int_{\Omega} \epsilon_{ijk} \epsilon_{ilm} \hat{u}_{k,j}^{*N} \hat{u}_{m,l}^{*N} d\Omega$$

The unperturbed mode shapes $\hat{\xi}_i^N$ and the wave number k_N are calculated from the homogeneous equations

$$\frac{i}{R_e} \hat{\xi}_{i,jj}^{*N} + k \hat{\xi}_i^{*N} = 0 \quad (46)$$

$$\hat{\xi}_{i,j}^{*N} n_j = 0 \quad (47)$$

The vorticity growth constant α_v can be derived by the relation (18) and (45),

$$\alpha_v = -\frac{1}{D_N^2} \int_{\Omega} \epsilon_{ijk} \epsilon_{kmn} (\bar{u}_m \hat{\xi}_n^{*N} + \hat{u}_m^{*N} \bar{\xi}_n) \hat{\xi}_{i,j}^{*N} d\Omega \quad (48)$$

Note that the term associated with acoustic fluctuation velocity \hat{u}_k in Eq. (44) drops out as a result of squaring the imaginary number which appears also in Eq. (38), thus making this term a real part. If desired for a computational standpoint, we may replace the vorticity in terms of velocity,

$$\hat{\xi}_i^{*N} = \epsilon_{ijk} \hat{u}_{k,j}^{*N}, \quad (49a)$$

$$\bar{\xi}_i = \epsilon_{ijk} \bar{u}_{k,j} \quad (49b)$$

Evaluation of Eq. (46) or Eq. (48) is now straightforward once the mean flow \bar{u}_i and fluctuating velocity \hat{u}_i^{*N} or the vorticity ξ_i^{*N} can be numerically determined using the finite element method. The hyperbolic tangent velocity profile for the mean flow and shear layers [9-12] may be used for one-dimensional integration.

The growth rate for the vortex shedding α_v represents an independent vorticity instability equivalent to the solution of Orr-Sommerfeld equation. When vortex shedding frequency approximates the classical acoustic frequency, periodic flow separations can produce significant pressure oscillations. To this end we perform the eigenvalue analyses for both Eqs. (24) and (46) and we enter the results into Eq. (31).

4. FINITE ELEMENT ANALYSIS

The use of finite elements in fluid mechanics problems has increased significantly in recent years. An application of this method to combustion instability was first studied in [7]. Our current effort is directed toward extending the work of [7] to incorporate the new terms in the stability integral as described in Section 3.

To begin we return to a classical acoustic problem characterized by Eq. (24) and Eq. (25). The Galerkin finite element equation takes the

form [13],

$$\int_{\Omega} (p_{,ii} + k^2 p) \phi_{\alpha} d\Omega = 0 \quad (50)$$

where ϕ_{α} is the test function which is set equal to the trial (basis) function such that

$$p(\underline{x}, t) = \phi_{\alpha}(\underline{x}) p_{\alpha}(t) \quad (51)$$

Here \underline{x} and t denote spatial and temporal variations, respectively, the subscript α representing the global node number with $\alpha = 1, 2, \dots, n$, n being the total number of global nodes.

It follows from Eq. (50) that the finite element eigenvalue equation is of the form

$$\left| A_{\alpha\beta} - k^2 B_{\alpha\beta} \right| = 0 \quad (52)$$

where

$$A_{\alpha\beta} = \int_{\Omega} \phi_{\alpha,i} \phi_{\beta,i} d\Omega, \quad B_{\alpha\beta} = \int_{\Omega} \phi_{\alpha} \phi_{\beta} d\Omega \quad (53)$$

The normal modes \hat{p}_N required for the stability integral can then be determined from Eq. (51). Non-axisymmetric geometries for slots, segments or irregular flow domain are modeled routinely using the Fourier series expansion [7].

Similarly, the vorticity transport Eq. (40) is cast in the form

$$\left| A_{\alpha\beta}^{ik} - k B_{\alpha\beta}^{ik} \right| = 0 \quad (54)$$

where

$$A_{\alpha\beta}^{ik} = \frac{i}{\text{Re}} \int_{\Omega} \phi_{\alpha,j} \phi_{\beta,j} \delta_{ik} d\Omega, \quad B_{\alpha\beta}^{ik} = \int_{\Omega} \phi_{\alpha} \phi_{\beta} \delta_{ik} d\Omega \quad (55)$$

The well-known QR algorithm [14] is invoked for the solution of eigenvalues and eigenvectors. As a result, the normal modes $\hat{\xi}_i^{*N}$ or \hat{u}_i^{*N} are calculated and substituted into the stability integrals, Eq. (31) and Eq. (48).

Once the normal modes are determined either numerically or analytically, the evaluation of stability integrals by finite elements is most appealing. Highly nonlinear, complicated functions can be integrated quite accurately via Gaussian quadrature, using the isoparametric finite elements [13].

For example, the stability integral is written in the form

$$\alpha = \int_{\Omega} F(\underline{x}) d\Omega = \int_{-1}^1 \int_{-1}^1 \int_{-1}^1 G(\xi, \eta, \zeta) d\xi d\eta d\zeta \quad (56)$$

This leads to the Gaussian quadrature process,

$$\alpha = \sum_{i=1}^m \sum_{j=1}^m \sum_{k=1}^m w_i w_j w_k G(\xi_i, \eta_j, \zeta_k) \quad (57)$$

where the weighting functions w_i, w_j, w_k and abscissae ξ_i, η_j, ζ_k are chosen for an adequate number of Gaussian points.

5. APPLICATIONS

5.1 General

The stability integrals given in Section 3 and the finite element equations as shown in Eq. (57) will be discussed. We begin with boundary conditions defined on the burning surface (Γ_b) and the nozzle entrance (Γ_n) as represented by the admittance functions:

$$A_b = - \frac{u'_i n_i}{\bar{M}_b p' / \gamma} \quad \text{on } \Gamma_b \quad (58)$$

$$A_n = \frac{u'_i n_i}{\bar{M}_n p' / \gamma} \quad \text{on } \Gamma_n \quad (59)$$

where \bar{M}_b and \bar{M}_n are the mean flow Mach numbers on Γ_b and Γ_n , respectively.

At this point, it is important to realize that the different forms of convective terms in the momentum equation would give different results for combustion instability phenomena,

$$\text{Case 1: } \nabla \left(\frac{1}{2} u^2 \right) - \underline{u} \times \underline{\xi} \quad (60)$$

$$\text{Case 2: } (\underline{u} \cdot \nabla) \underline{u} \quad (61)$$

The difference is particularly significant when dominated by vortex sheddings. To see this, we rewrite Eq. (23) in terms of admittance functions for the Cases 1 and 2, respectively,

Case 1:

$$\alpha = \alpha_a + \alpha_H \quad (62)$$

where

$$\begin{aligned} \alpha_a = & -\frac{1}{2E_N^2} \left[-A_b^{(R)} \bar{M}_b \int_{\Gamma_b} \hat{p}_N^2 d\Gamma_b + A_n^{(R)} \bar{M}_n \int_{\Gamma_n} \hat{p}_N^2 d\Gamma_n + \frac{1}{k_N^2} \int_{\Gamma} \bar{u}_j \hat{p}_{N,j} \hat{p}_{N,i} n_i d\Gamma \right. \\ & + (\gamma+1) \int_{\Gamma} \bar{u}_i \hat{p}_N^2 n_i d\Gamma - \frac{1}{k_N^2 \text{Re}} \int_{\Gamma} (\hat{p}_{N,i} \hat{p}_{N,ij} n_j + \frac{1}{3} \hat{p}_{N,i} \hat{p}_{N,jj} n_i) d\Gamma \\ & + \int_{\Omega} \left\{ -\bar{u}_{i,i} \hat{p}_N^2 - (2\gamma+1) \bar{u}_i \hat{p}_N \hat{p}_{N,i} - \frac{1}{k_N^2} \left[\bar{u}_j \hat{p}_{N,j} \hat{p}_{N,ii} \right. \right. \\ & \left. \left. + \epsilon_{ijk} \bar{\xi}_k \hat{p}_{N,i} \hat{p}_{N,j} \right] + \frac{1}{k_N^2 \text{Re}} \left(\hat{p}_{N,ij} \hat{p}_{N,ij} + \frac{1}{3} \hat{p}_{N,ii} \hat{p}_{N,jj} \right) \right\} d\Omega \end{aligned} \quad (63a)$$

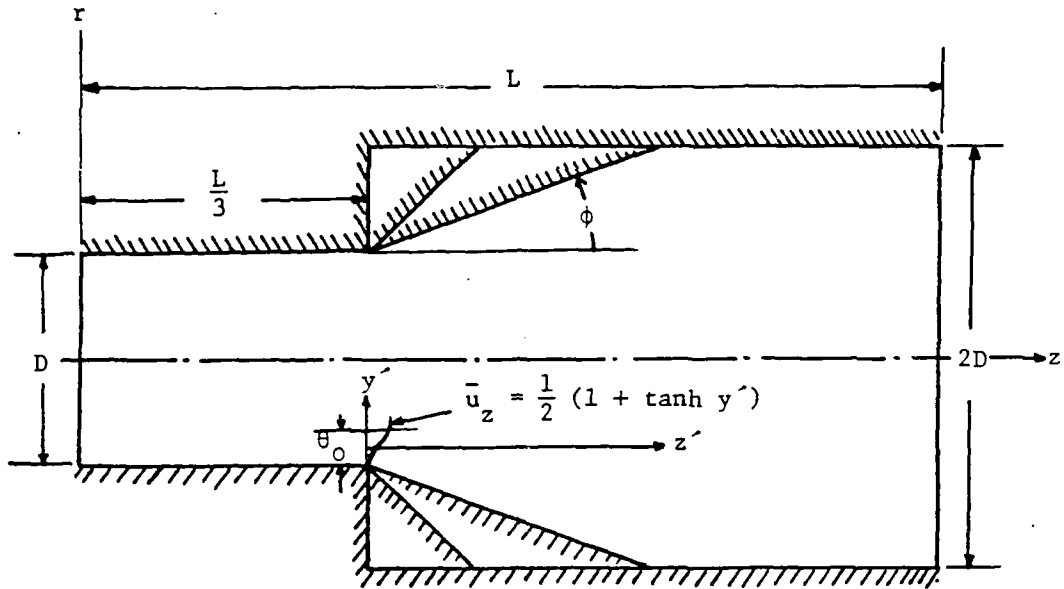
$$\begin{aligned} \alpha_H = & -\frac{1}{2E_N^2} \left[\int_{\Gamma} \left\{ \frac{\gamma}{k_N} \bar{u}_j \hat{u}_j^{*(I)} \hat{p}_{N,i} n_i - \frac{\gamma}{k_N \text{Re}} \left(\hat{u}_{i,j}^* \hat{p}_{N,i} n_j + \frac{1}{3} \hat{u}_{j,j}^{*(I)} \hat{p}_{N,i} n_i \right) \right\} d\Gamma \right. \\ & + \int_{\Omega} \left\{ -\frac{\gamma}{k_N} \left[\bar{u}_j \hat{u}_j^{*(I)} \hat{p}_{N,ii} + \epsilon_{ijk} \left(\bar{u}_j \hat{\xi}_k^{(I)} + \hat{u}_j^{*(I)} \bar{\xi}_k \right) \hat{p}_{N,i} \right] \right. \\ & \left. + \frac{\gamma}{k_N \text{Re}} \left(\hat{u}_{i,j}^*(I) \hat{p}_{N,ij} + \frac{1}{3} \hat{u}_{j,j}^*(I) \hat{p}_{N,ii} \right) \frac{2\gamma(\gamma-1)}{\text{Re}} \left(\frac{2}{3} \bar{u}_{i,i} \hat{u}_{j,j}^{*(R)} \right. \right. \\ & \left. \left. - \bar{u}_{i,j} \hat{u}_{j,i}^{*(R)} - \bar{u}_{j,i} \hat{u}_{j,i}^{*(R)} \right) \hat{p}_N \right\} d\Omega \end{aligned} \quad (63b)$$

Case 2:

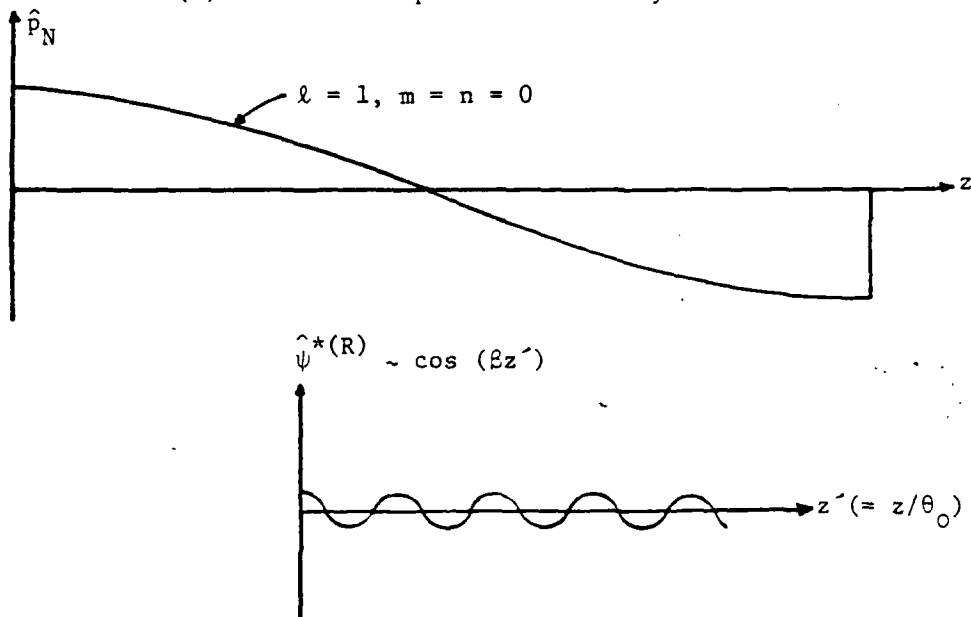
$$\begin{aligned}
 \alpha_a = & -\frac{1}{2E_N^2} \left[\underbrace{-A_b^{(R)} \bar{M}_b \int_{\Gamma_b} \hat{p}_N^2 d\Gamma_b + A_n^{(R)} \bar{M}_n \int_{\Gamma_n} \hat{p}_n^2 d\Gamma_n}_{(A-1)} \right. \\
 & - \underbrace{(\gamma+1) \int_{\Gamma} \bar{u}_i \hat{p}_N^2 n_i d\Gamma}_{(A-2)} + \underbrace{\frac{1}{k_N^2} \int_{\Gamma} (\bar{u}_j \hat{p}_{N,i} \hat{p}_{N,i} n_j + \bar{u}_i \hat{p}_{N,i} \hat{p}_{N,j} n_j)}_{(B-1)} d\Gamma \\
 & - \underbrace{\frac{1}{k_N^2 \text{Re}} \int_{\Gamma} (\hat{p}_{N,i} \hat{p}_{N,ij} n_j + \frac{1}{3} \hat{p}_{N,jj} \hat{p}_{N,ii} n_i)}_{(C)} d\Gamma + \int_{\Omega} \left\{ \underbrace{-\bar{u}_{i,i} \hat{p}_N^2}_{(D-1)} - \underbrace{(2\gamma+1) \bar{u}_i \hat{p}_N \hat{p}_{N,i}}_{(D-2)} \right. \\
 & - \frac{1}{k_N^2} \left(\underbrace{\bar{u}_i \hat{p}_{N,jj} \hat{p}_{N,i}}_{(E-1)} + \underbrace{\bar{u}_{j,j} \hat{p}_{N,i} \hat{p}_{N,i}}_{(E-2)} + \underbrace{\bar{u}_i \hat{p}_{N,j} \hat{p}_{N,ij}}_{(E-3)} \right. \\
 & \left. \left. + \underbrace{\bar{u}_j \hat{p}_{N,i} \hat{p}_{N,ij}}_{(E-4)} + \frac{1}{k_N^2 \text{Re}} \left(\hat{p}_{N,ij} \hat{p}_{N,ij} + \frac{1}{3} \hat{p}_{N,ii} \hat{p}_{N,jj} \right) \right\} d\Omega \right] \quad (64a)
 \end{aligned}$$

$$\begin{aligned}
 \alpha_H = & -\frac{1}{2E_N^2} \left[\int_{\Gamma} \left\{ \frac{\gamma}{k_N} [\bar{u}_i \hat{u}_j^{*(I)} + \hat{u}_j^{*(I)} \bar{u}_j] \hat{p}_{N,i} - \frac{\gamma}{k_N \text{Re}} [\hat{u}_{i,j}^* \hat{p}_{N,ij} n_j \right. \right. \\
 & \left. \left. + \frac{1}{3} (\hat{u}_{j,j}^* \hat{p}_{N,ii} n_i) \right\} d\Gamma + \int_{\Omega} \left\{ -\frac{\gamma}{k_N} \left(\bar{u}_i \hat{u}_{j,j}^{*(I)} \hat{p}_{N,i} + \bar{u}_{j,j} \hat{u}_i^{*(I)} \hat{p}_{N,i} \right. \right. \\
 & \left. \left. + \bar{u}_i \hat{u}_j^{*(I)} \hat{p}_{N,ij} + \bar{u}_j \hat{u}_i^{*(I)} \hat{p}_{N,ij} \right) + \frac{\gamma}{k_N \text{Re}} \left(\hat{u}_{i,j}^{*(I)} \hat{p}_{N,ij} \right. \right. \\
 & \left. \left. + \frac{1}{3} \hat{u}_{j,j}^{*(I)} \hat{p}_{N,ii} \right) + \frac{2\gamma(\gamma-1)}{\text{Re}} \left(\frac{2}{3} \bar{u}_{i,i} \hat{u}_{j,j}^{*(R)} - \bar{u}_{i,j} \hat{u}_{j,i}^{*(R)} \right. \right. \\
 & \left. \left. - \bar{u}_{j,i} \hat{u}_{j,i}^{*(R)} \right) \hat{p}_N \right\} d\Omega \quad (64b)
 \end{aligned}$$

Here α_H denotes the coupling of vortical velocity fluctuations \hat{u}_i^* and the local acoustic pressure \hat{p}_N .



(a) Conical Shape Grain Geometry



(b) Vortical Fluctuations Coupled with the Acoustic Field \hat{p}_N

Figure 1 A Physical Model of the Problem

5.2 Vorticity-Uncoupled Acoustic Instability

We consider the axisymmetric conical geometry (Figure 1a) with a transitional angle ϕ and a port diameter D which diverges into $2D$ at the nozzle entrance, the transition beginning at $z=L/3$. It is assumed that $a\bar{M}_b = 10$ in/sec, $\gamma = 1.2$, and $\nu = 0.1$ in²/sec. It is further assumed that the mean flow velocity is given by [16],

$$\bar{u}_i = \bar{M}_b \left[-\frac{R}{r} \sin\left(\frac{\pi r^2}{2R^2}\right) \hat{e}_r + \frac{\pi z}{R} \cos\left(\frac{\pi r^2}{2R^2}\right) \hat{e}_z \right] \quad (65)$$

where R is the radius as a function of z and \hat{e}_r and \hat{e}_z are unit vectors in the radial and axial directions, respectively.

The classical acoustic modes \hat{p}_N are given by the formulas

$$\hat{p}_N = \cos(k_\ell z) \cos(m\theta) J_m(k_{mn} r) \quad (66)$$

with

$$k_N^2 = k_\ell^2 + k_{mn}^2 \quad (67)$$

where $m = 0, 1, 2, \dots$, $k_\ell = \ell\pi/L$ with $\ell = 0, 1, 2, \dots$, and k_{mn} are the roots of

$$\frac{d}{dr} J_m(k_{mn} r) = 0 \text{ at } r = R(z)$$

To evaluate α_a in Eq. (64a), the vorticity-uncoupled growth rate, we make use of Eqs. (65-67), rewrite Eq. (64a) in terms of finite elements, and transform the integrand into the form of Eq. (57). To demonstrate the accuracy of calculations we choose the results of terms given by (A-2) and (B-1) which are shown in Table 1. Here we used 4×4 Gaussian points, $\phi = 0$, $L/D = 1$, $A_b^{(R)} = 1$, $A_n^{(R)} \bar{M}_n / \bar{M}_b = 1$. A comparison with analytical calculations indicates an excellent agreement.

Mode (lmn)	$\alpha_{(A-2)}$		$\alpha_{(B-1)}$	
	Analytical	Present Study	Analytical	Present Study
(100)	-4.400	-4.400	2.000	2.000
(200)	-4.400	-4.400	2.000	2.000
(010)	-6.253	-6.253	0.849	0.848
(110)	-6.253	-6.253	1.683	1.683

Table 1. Acoustic Instability Growth Rate - Integrals (A-2) and (B-1) in Eq. (64a).

Figure 2 shows the acoustic instability growth rate α_a versus the transition angle ϕ for several modes. It is interesting to note that, for both Case 1 and Case 2, the tangential mode tends to be more unstable in comparison with other modes, and that instability increases with larger transition angles. However, for a given mode, Case 1 exhibits more instability than Case 2. To the best of our knowledge this has not been brought to the attention of the combustion community [17]. Furthermore, it has been demonstrated in Table 2 that the effect of viscosity (C+F) is negligible in the cylinder of uniform diameter (no flow separation).

It should be noted that an alternative approach is to perform the eigenvalue analysis for Eq. (52). The acoustic modes \hat{p}_N are then calculated and used in the evaluation of stability integral. For irregular geometries (non-axisymmetric) such as occur in the star-shaped propellants we must resort to the eigenvalue analysis. Numerical results using the procedure as employed in [7] are forthcoming in a subsequent paper.

Integrals Mode (l,m)		Integrals					
		A	B	C	D	E	F
(001)	Case 1	-.0762	0.0	-.0000	.6793	-.1998	-.0421
	Case 2	-.0762	-3.7400	-.0000	.6793	-.5994	-.0421
(010)	Case 1	5.3288	0.0	0.0024	-2.3040	0.6777	-.1102
	Case 2	5.3288	0.0	0.0024	-2.3040	-1.953	-.1102
(100)	Case 1	-7.0292	0.0	0.0061	6.4790	-1.9060	-.0221
	Case 2	-7.0292	2.9130	0.0061	6.4790	-7.561	-.0221
(110)	Case 1	-1.4362	0.0	0.0035	2.9720	-.9740	-.1144
	Case 2	-1.4362	-5.0640	0.0035	2.9720	0.3971	-.0225
(200)	Case 1	-4.8580	0.0	0.0060	4.1420	-1.2180	-.0225
	Case 2	-4.8580	2.1220	0.0060	4.1420	-5.060	-.0225

Table 2. Growth Rates for $\frac{L}{D} = 4$, $\phi = \frac{\pi}{4}$, Eq. 64a.

5.3 Vorticity-Coupled Instability

A complete three-dimensional analysis for the vorticity-coupled instability must follow the eigenvalue analysis as required by Eq. (54).

The vortical modes $\hat{\xi}_i^N$ and disturbances \hat{u}_i^{*N} thus calculated may be substituted into α_H in Eq. (63b) or Eq. (64b). Similar calculations for Eq. (47) can be carried out for the case of an acoustic-uncoupled vorticity instability.

In this paper, however, it is our plan not to be involved in the eigenvalue analysis but to show an analytical approach using the hyperbolic tangent velocity profile for a shear layer [10-12]. Here we assume the stream function $\psi^*(r,z,t)$ representing a single oscillation

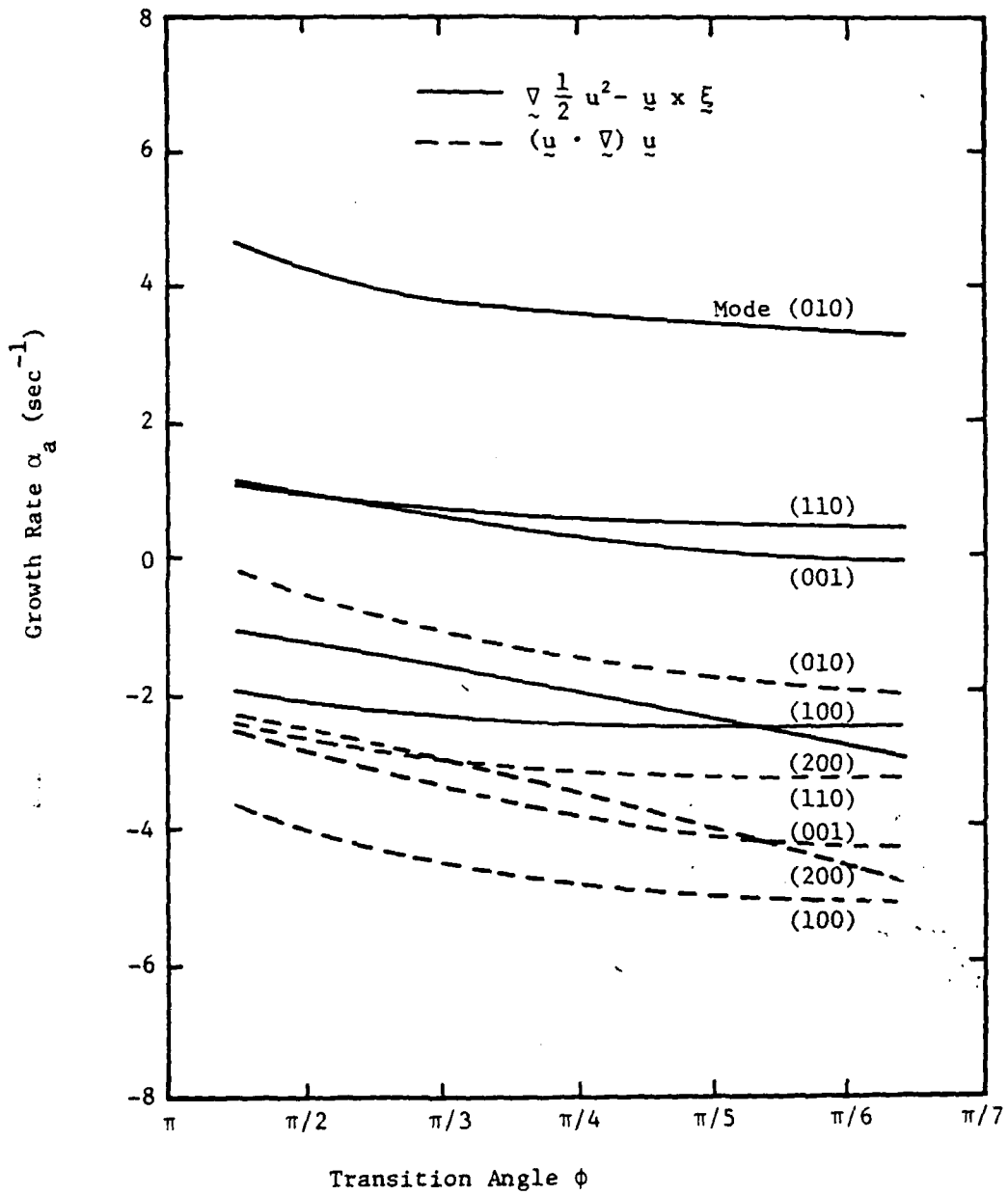


Figure 2 The Acoustic Growth Rates α_a Vs. Transition Angles for Different Modes, $L/D = 4$ and $a\bar{M}_b = 10$ in/sec.

of a disturbance to be of the form [9].

$$\psi^*(r, z, t) = \hat{\psi}^*(r, z) e^{ikt} \quad (68)$$

where k is the complex dimensionless frequency defined in Eq. (18). We further assume that the disturbance amplitude of the stream function $\hat{\psi}^*(r, z)$ has the same form as in [10]

$$\hat{\psi}^*(r, z) = e^{-\mu y'} e^{i\beta z'} \quad (69)$$

where μ and β are real quantities representing the various mode shapes which may depend on the geometry, and y' and z' are the coordinates normalized with respect to the boundary layer thickness θ_0 at the separation point ($z' = 0$) and measured from the inflection point as shown in Figure 1a. That is, the disturbance effect of vortex shedding on the acoustic field is assumed to begin at the critical point ($z' = 0$) and vanish downstream before entering the nozzle. Figure 1b shows the disturbance function $\hat{\psi}^{*(R)}$ coupled with the acoustic field \hat{p}_N for a longitudinal mode. The velocity disturbances \hat{u}_z^* and \hat{u}_r^* for an incompressible axisymmetric flow are given by

$$\hat{u}_z^* = \frac{1}{r} \frac{\partial \hat{\psi}^*}{\partial r}, \quad \hat{u}_r^* = -\frac{1}{r} \frac{\partial \hat{\psi}^*}{\partial z} \quad (70)$$

The mean flow representing a hyperbolic tangent velocity profile [10-12] assumes the form

$$\hat{u}_z = \frac{1}{2} (1 + \tanh y') \quad (71)$$

The shear layer thickness θ_0 is found experimentally to be a function of

μ	β	α_H (sec ⁻¹)		α_V (sec ⁻¹)
		$\ell=1, m=n=0$	$\ell=2, m=n=0$	
0.2	0.2	92.919	-132.770	-6.437
		105.043	-108.990	
	0.6	30.522	- 42.930	5.135
34.493		- 54.611		
1.0	0.334	3.198	-0.000	
	2.137	- 2.869		
0.6	0.2	85.758	-125.730	-2.059
		97.814	-102.746	
	0.6	28.168	- 40.050	14.789
32.116		- 52.588		
1.0	0.426	2.136	-0.000	
	2.315	- 4.244		
1.0	0.2	78.260	-117.662	-2.360
		95.345	-160.654	
	0.6	25.704	- 38.040	4.025
31.305		- 51.912		
1.0	0.465	1.246	-0.000	
	2.259	- 4.543		

Table 3. Growth Rates α_H and α_V , the Upper Numbers are for Case 1 and the Lower Numbers for Case 2, $\phi = \pi/2$.

Reynolds numbers and the jet diameters,

$$\theta_o = \frac{cD}{\sqrt{\text{Re}}(S)} \quad (72)$$

where

$$\text{Re}^{(S)} = U_o D/\nu \quad (73)$$

with U_o being the free stream velocity, and $c_o \approx 0.62$ for cylindrical geometries [12].

For various vortical mode shape combinations of μ and β the growth rates α_H and α_V are calculated for the two first longitudinal modes (Table 3). Here the same physical constants are used as in Figure 1 with $\phi = \pi/2$. Note that α_V is independent of the acoustic mode and $\alpha_H = 0$ for any tangential modes. The results indicate that α_H is strongly dependent on β while slightly dependent on μ for the two longitudinal modes, and that the higher mode is more stable than the lower one. Note also that the trend of α_V is similar to that of α_H but α_V has the largest instability occurring at $\beta = 0.6$, and neutral stability at $\beta = 1$ for all μ 's. For the first longitudinal mode, the values of α_H are in the range of the case investigated in [9].

6. CONCLUSIONS

A significant improvement over the current practice of combustion stability calculations is achieved. A three-dimensional formulation of stability integral for the coupled acoustic-vortex fluctuations leads to new integral terms accounting for the various phenomena previously neglected.

One of the terms in three-dimensional combustion instability integral, identified as "flow-turning", was shown to be the result of integrating by parts, twice, one of the convective terms of the momentum equation. The most crucial factor is the correct procedure for integration by parts which will affect the accuracy in determining the instability. It has been shown that in a three-dimensional case, the use of tensorial approach is more efficient than the vector notations.

The viscosity effect is small as expected for the uniform cylinder. However, it will contribute greatly if the geometry becomes irregular.

A new vortical instability integral is derived, which represents the classical hydrodynamic instability. This avoids solution of the three-dimensional Orr-Sommerfeld equation. A simple case of hyperbolic tangent velocity profile is used for shear layer instability calculations. In the case of an acoustic-coupled vortical instability, it is noted that no contribution results from tangential modes.

In this study, we utilize an analytical form of classical normal modes for the cylindrical acoustic field. For irregular geometries, however, we must resort to the standard eigenvalue analysis to obtain the acoustic and vortical mode shapes and frequencies. With such data we return to the stability integral and proceed identically as shown in the simple examples given in this paper.

References

1. Crocco, L. and Chen, S. I., "Theory of Combustion Instability in Liquid Propellant Rocket Motors," AGARDograph No. 8, Butterworth Scientific Publication, London, 1956.
2. Cantrell, R. H. and Hart, R., "Interaction Between Sound and Flow in Acoustic Cavities: Mass, Momentum, and Energy Considerations," Journal of the Acoustical Society of America, Vol. 36, April, 1964, pp. 697-706.
3. Culick, F. E. C., "The Stability of One-Dimensional Motions in a Rocket Motor," Vol. 7, 1973, pp. 165-175.
4. Culick, F. E. C., "Stability of Three-Dimensional Motions in a Combustion Chamber," Comb. Sci. and Tech., Vol. 10, 1975, pp. 109-124.
5. Flandro, G. A. and Jacobs, H. P., "Vortex Generated Sound in Cavities," Progress in Aeronautics and Astronautics, Vol. 37, AIAA, 1975, pp. 521-533.
6. Flandro, G. A., "Stability Prediction for Solid Propellant Rocket Motors with High Speed Mean Flow," AFRPL-TR-79-98, 1980.
7. Hackett, R. M., "Three-Dimensional Finite-Element Acoustic Analyses of Solid Rocket Motor Cavities," Journal of Space Craft and Rockets, Vol. 13, No. 10, 1976, pp. 585-588.
8. Morse, P. M. and Feshbach, H., Methods of Theoretical Physics, Part I and II, McGraw-Hill Book Co., 1953.
9. Brown, R. S., Dunlap, R., Young, S.W., Flandro, G. A., Isaacson, L. K., Beddini, R. A., and Culick, F. E. C., "Vortex Shedding Studies," AFRPL-TR-80-13, April, 1980.
10. Michalke, A., "On Spatially Growing Disturbances in an Inviscid Shear Layer," Journal of Fluid Mechanics, Vol. 23, Part 3, 1965, pp. 521-554.
11. Michalke, A., "On the Inviscid Instability of the Hyperbolic-Tangent Velocity Profile," Journal of Fluid Mechanics, Vol. 19, Part 3, 1964, pp. 543-556.
12. Freymuth, P., "On Transition in a Separated Liminar Boundary Layer," Journal of Fluid Mechanics, Vol. 25, Part 4, 1966, pp. 683-704.
13. Chung, T. J., Finite Element Analyses in Fluid Dynamics, McGraw-Hill Book Co., 1978.
14. Wilkinson, J. H., The Algebraic Eigenvalue Problem, Clarendon Press, Oxford, 1965.

15. Dong, S. B., "A Block-Stodola Eigensolution Technique for Large Algebraic Systems with Nonsymmetrical Matrices," Int. J. for Numerical Meth. in Eng., Vol. 1, 11, 1977, pp. 247-267.
16. Culick, F. E. C., "Rotational Axisymmetric Mean Flow and Damping of Acoustic Waves in a Solid Propellant Rocket," AIAA J., Vol. 4, No. 8, August, 1966.
17. Lovine, R. L., "Standard Stability Prediction Method for Solid Rocket Motors," AFRPL-TR-76-32, Aerojet Solid Propulsion Co., May, 1976.

DISTRIBUTION

	No. of Copies
Defense Documentation Center Cameron Station Alexandria, Virginia 22314	12
IIT Research Institute ATTN: GACIAC 10 West 35th Street Chicago, Illinois 60616	1
US Army Material Systems Analysis Activity ATTN: DRXS-MP Aberdeen Proving Ground, Maryland 21005	2
CPIA Distribution	96
Air Force Rocket Propulsion Laboratory ATTN: DYSC/Mr. W. Roe Mr. J. Levin Edwards, California 93523	1 1
Hercules, Inc. ATTN: Mr. N. Peterson P. O. Box 98 Magna, Utah 84044	1
Chemical Systems Division United Technologies ATTN: Dr. R. S. Brown Mr. R. Waugh Sunnyvale, California 94088	1 1
California Institute of Technology ATTN: Dr. F. E. C. Culick 204 Karman Laboratory/Mail No. 301-46 1201 East California Pasadena, California 91109	1
Naval Weapons Center Aerothermochemistry Division ATTN: Code 608, Dr. R. L. Derr Mr. B. Matthes Mr. C. J. Bicker China Lake, California 93555	1 1 1

DISTRIBUTION

	No. of Copies
California State University Department of Mechanical Engineering ATTN: Dr. F. Reardon Sacramento, California 95819	1
Georgia Institute of Technology Department of Aerospace Engineering ATTN: Dr. E. W. Price Dr. B. T. Zinn Atlanta, Georgia 30332	1 1
Rockwell International Corporation Rocketdyne Division ATTN: Mr. W. T. Brooks P. O. Box 548 McGregor, Texas 76657	
NASA-Marshall Space Flight Center ATTN: Mr. B. Shackelford Mr. C. Forsythe EP25 Huntsville, Alabama 35812	1 1
Aerojet Solid Propulsion Company ATTN: Mr. R. L. Lovine Building 2019/Department 4350 P. O. Box 13400 Sacramento, California 95813	1
University of Utah Department of Mechanical Engineering ATTN: Dr. G. A. Flandro Salt Lake City, Utah 84112	1
Thiokol Chemical Corporation Wasatch Division ATTN: Dr. C. M. Milfeith Mr. S. Folkman P. O. Box 524 Brigham City, Utah 94302	1 1
Thiokol Chemical Corporation Huntsville Division ATTN: Dr. R. Kruse Mr. R. Hessler Mr. G. Estes Huntsville, Alabama 35807	1 1 1

DISTRIBUTION

	No. of Copies
Princeton University Department of Aerospace and Mechanical Science ATTN: Dr. W. A. Sirignano P. O. Box 710 Princeton, New Jersey 08540	1
Commander US Army Materiel and Readiness Command ATTN: DRCRD DRCDL 5001 Eisenhower Avenue Alexandria, Virginia 22333	1 1
Battelle Columbus Laboratories Durham Office P. O. Box 8796 Durham, North Carolina 27707	1
Hercules, Inc. Allegany Ballistics Laboratory ATTN: Mr. J. Murray P. O. Box 210 Cumberland, Maryland 21502	1
DRSMI-FM, Mr. Little	1
DRSMI-LP, Dr. Garvin	1
DRSMI-X	1
DRSMI-R, Dr. McCorkle	1
DRSMI-R, Dr. Rhoades	1
DRSMI-R, Mr. Black	1
DRSMI-RKK	1
DRSMI-RKA	10
DRSMI-RKP	1
DRSMI-RKC	1
DRSMI-RPR	5
DRSMI-IYB	1
DRSMI-RPT (Record Copy)	1
(Reference Copy)	1

ATE
LME
8